ACS Catalysis

Letter

pubs.acs.org/acscatalysis

Multiscale Model for a Metal−Organic Framework: High-Spin Rebound Mechanism in the Reaction of the Oxoiron(IV) Species of Fe-MOF-74

Hajime Hirao,* Wilson Kwok Hung Ng, Adhitya Mangala Putra Moeljadi, and Sareeya Bureekaew

Division of Chemistry and Biological Chemistry, School of Physical and Mathematical Sciences, Nanyang Technological University, 21 Nanyang Link, Singapore 637371

Supporting Information

ABSTRACT: We performed ONIOM QM/MM calculations to understand how ethane is hydroxylated and ethanol is converted to acetaldehyde by an oxoiron(IV) species generated within an iron-containing metal−organic framework called Fe-MOF-74. The calculations showed that the ethane hydroxylation proceeds via a high-spin rebound mechanism. The conversion of ethanol into acetaldehyde should occur more favorably via H-abstraction from the O−H bond than via C−H cleavage, although the O−H bond of ethanol is stronger than the C(1)−H bond. This trend can be rationalized by the effect of proton-coupled electron transfer, which stabilizes the transition state for O−H cleavage.

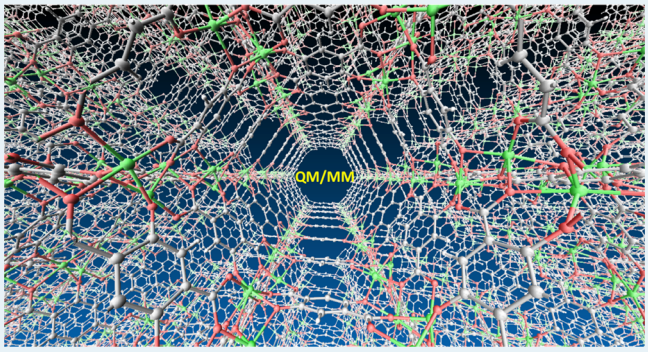

KEYWORDS: *metal−organic framework, oxoiron(IV), QM/MM, C−H activation, PCET*

The high-valent oxoiron(IV) active species plays crucial roles in the enzyme catalysis of alkane hydroxylation, olefin epoxidation, and other types of oxidation reactions occurring in heme and non-heme iron enzymes.[1,2] For example, cytochrome P450 enzymes (P450s) are representative of the heme enzymes that utilize oxoiron(IV) for catalysis,[3−5] and taurine:α-ketoglutarate dioxygenase (Tau-D) is often cited as an exemplary case in which oxoiron(IV) is generated and used in a non-heme iron enzyme.[2] Traditionally, the oxoiron(IV) porphyrin π-cation radical species of P450s is called Cpd I, and the oxoiron(IV) species of Tau-D is termed TauD-J. The remarkable oxidative reactivity of Cpd I has inspired synthetic efforts to prepare oxoiron(IV) porphyrin complexes.[6−8] Substantial efforts have also been devoted to the synthesis and characterization of biomimetic oxoiron(IV) supported by non-heme ligands,[8−13] especially since the first isolation of a synthetic non-heme oxoiron(IV) complex.[10]

In addition to the experiments, many computational studies have been undertaken. The previous computational studies have elucidated the electronic details of various oxoiron(IV) species and thereby helped advance our understanding of their reactivity trends.[14] For example, density functional theory (DFT) studies performed by one of us (H.H.) and Shaik predicted that high-spin states (sextet or quintet) of oxoiron(IV) species of P450s and synthetic non-heme complexes should have lower-barrier energy surfaces than low-spin states because there is enhancement of exchange stabilization at the iron center in the reactions of high-spin states.[14−17] Although the strong ligand field in P450 Cpd I might render the low-barrier, high-spin energy surface hard to access, this computationally derived scenario hinted that, if a high-spin oxoiron(IV) is stable enough to participate in a reaction, an essentially difficult chemical transformation may become easier. Synthetic non-heme oxoiron(IV) complexes also tend to have low-spin ground states, and thus, synthetic realization of their high-spin versions has been a difficult challenge. Nevertheless, several high-spin complexes have been synthesized by skillful experimentalists.[18−21] Furthermore, a reactive high-spin oxoiron(IV) species has recently been synthesized and characterized.[12]

Meanwhile, metal−organic frameworks (MOFs) (also called porous coordination polymers) have emerged as another important class of molecular systems that can use iron or other metals for heterogeneous catalysis.[22−27] The inner pores of these materials affect reaction selectivies,[28] and notably, the size and shape of the pores can be changed by varying the organic linkers and metal nodes used. In addition, if the numerous metal centers existing in a single MOF are used simultaneously for catalysis, the catalytic efficiency will become very high. Another attractive feature of MOFs is that redox-active metals can be utilized as metal nodes. Redox-active metals may exhibit behavior analogous to that in metalloenzymes, possibly conferring powerful enzyme-like catalytic activity on MOFs. Such MOFs indeed exist. For example, Fe_2(dobdc) (dobdc^{4-} = 2,5-dioxido-1,4-benzenedicarboxylate),

Received: March 5, 2015
Revised: April 20, 2015
Published: April 22, 2015

DOI: 10.1021/acscatal.5b00475
ACS Catal. 2015, 5, 3287−3291

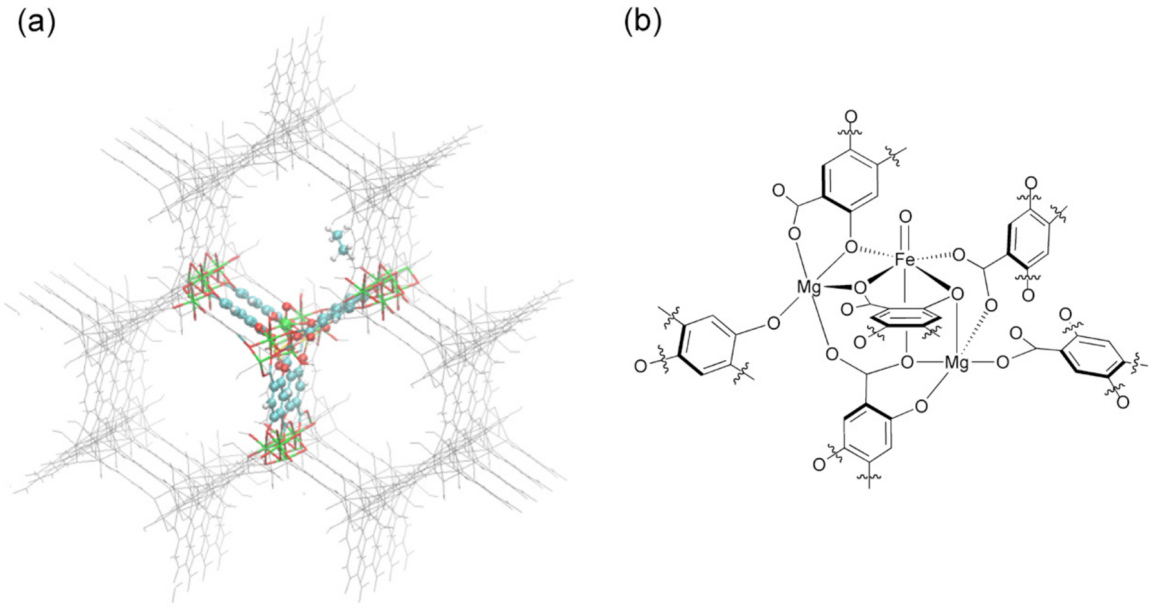

Figure 1. (a) The entire system used for our QM/MM study of ethane hydroxylation. The QM atoms are shown in ball-and-stick representation, and the atoms are shown in stick (for optimized atoms) and wire representations. (b) A schematic drawing of the QM region. A wavy line indicates a QM/MM boundary at which a H-link atom is attached on the QM side.

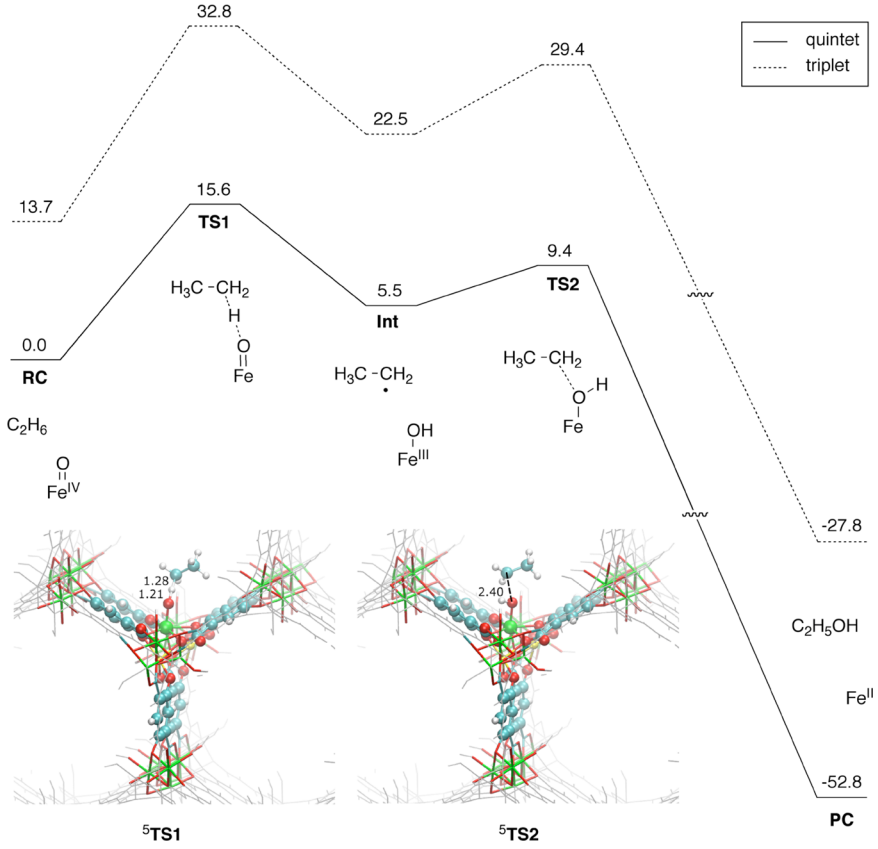

Figure 2. Potential energy profiles (in kcal/mol) for the reaction between ethane and the oxoiron(IV) species in the quintet and triplet states, as determined at the ONIOM(B3LYP/B2:UFF)//ONIOM(B3LYP/B1:UFF)+ZPE level. The optimized transition states in the quintet state are also depicted, and key distances are shown in Å.

also called Fe-MOF-74 or CPO-27-Fe, allows phenol hydroxylation,[29] conversion of methanol to formaldehyde,[30] oxidation of 1,4-cyclohexadiene, and hydroxylation of ethane[31] to proceed. Interestingly, Xiao et al. have recently proposed that a high-spin oxoiron(IV) species should be generated within Fe-MOF-74 and effects the hydroxylation of ethane; this reaction is unlikely to occur with other types of iron species, such as ferric hydroxide (Fe(III)OH), because ethane has very strong

DOI: 10.1021/acscatal.5b00475
ACS Catal. 2015, 5, 3287−3291

C−H bonds.[31] The weak ligand field in Fe-MOF-74 appears to provide an excellent environment for a high-spin oxoiron(IV).

As a continuation of our efforts to gain in-depth knowledge of oxoiron(IV), we wished to understand how the reactivity of oxoiron(IV) in Fe-MOF-74 differs from that of P450s and non-heme synthetic complexes. However, MOFs generally have remarkably high dimensionality in structure, the theoretical description of which may require multiscale models or hybrid quantum mechanics and molecular mechanics (QM/MM) calculations. Even though computational studies of chemical reactions in MOFs using QM/MM are still very scarce today in comparison with the numerous applications of QM/MM to enzymes,[32−36] QM/MM must have great potential for elucidating the catalytic mechanisms of MOFs containing oxoiron(IV) or any other reactive metal species. We herein attempt to apply QM/MM to the reactions of ethane and ethanol in Fe-MOF-74.

To build a QM/MM model, a published crystal structure of Fe-MOF-74, in which the iron center has an Fe(III)OH state, was modified (Figure 1).[31] Three Fe(III)OH ions were included in the QM region. The central Fe(III)OH was replaced with Fe(IV)O (Figure 1a), and this Fe(IV)O is to abstract hydrogen from a substrate. To simplify the electronic structure of the QM atoms, the other two Fe(III)OH units in the QM region were replaced with Mg(II) (Figure 1b). This simplification was based on the experimental observation that a magnesium-diluted analogue of Fe-MOF-74, that is, $Fe_{0.1}Mg_{1.9}$(dobdc), also showed catalytic activity.[31] The ONIOM method implemented in Gaussian09 was used for the QM/MM calculations.[37−40] The B3LYP/[SDD(Fe),6-31G*(others)] method was used for the QM atoms,[41−45] and the universal force field (UFF) was used for the MM calculations within ONIOM.[46] Zero-point vibrational energies (ZPEs) obtained from frequency calculations were included in the reported energy data. In addition to the above-mentioned basis set (B1), which was used for geometry optimization, the 6-311+G(df,p) basis set (B2) was also used for single-point energy calculations. G4 calculations were performed to evaluate the homolytic bond dissociation energies (BDEs) of ethane and ethanol.[47] Additional technical details can be found in the Supporting Information (SI).

Figure 2 shows the computationally determined energy diagrams for the hydroxylation of ethane. Unlike the reactions of P450 Cpd I and most of the synthetic non-heme oxoiron(IV) complexes, the high-spin state is more stable than the low-spin state at the stage of a reactant complex (RC). This trend is consistent with the computational results presented by Xiao et al.[31] Interestingly, the figure also shows that the quintet state is always the ground state throughout the reaction, which is distinctly different from the cases of many non-heme oxoiron(IV) complexes in which the triplet state is the ground state at the outset of the reaction.[17] Another interesting finding is that the barrier for H-abstraction is only 15.6 kcal/mol, despite the fact that the G4-calculated homolytic C−H BDE of ethane is as large as 100.7 kcal/mol (Table S2). This result suggests that the high-spin oxoiron(IV) species in Fe-MOF-74 can abstract hydrogen from ethane and supports Xiao et al.'s conclusion that the ethane hydroxylation should be effected by oxoiron(IV).[31] This calculated barrier height might contain some error because of the limited accuracy of B3LYP, but importantly, the high-spin reactivity was also predicted by two other DFT functionals (Figure S1). The H-abstraction via TS1 leads to the formation of an intermediate (Int) containing an ethyl radical and an Fe(III)OH species. The ethyl radical then undergoes a radical rebound via a transition state (TS2),[48] to form an alcohol product complex (PC). The resultant ferrous species in PC may be later converted to Fe(III)OH via a reaction with N_2O in the system.[31] It should be noted that although the calculated rebound barrier is low (3.9 kcal/mol), our calculation does not necessarily rule out the possibility that the ethyl radical attacks some other Fe(III)OH or Fe(IV)O unit within the MOF instead of attacking the Fe(III)OH at which H-abstraction from this substrate has taken place. This is because the position and orientation of the substrate are not tightly restricted in the pore space of the MOF (Figure 1a), and this situation is very different from that in enzyme active sites that generally have a high degree of shape complementarity to substrates. In fact, for the reaction of a synthetic non-heme oxoiron(IV) complex, which cannot anchor the substrate strongly to the reaction center, it has been shown that the substrate radical can dissociate from the Fe(III)OH after H-abstraction.[49]

The barrier heights for H-abstraction in the quintet and triplet states were calculated as 15.6 and 19.1 kcal/mol, respectively. The somewhat lower barrier obtained for the quintet state can be rationalized in terms of exchange enhancement at the iron center. Figure 3 shows changes in the atomic spin population values for Fe, O (oxygen of oxoiron(IV)), and C (carbon of ethane from which hydrogen is abstracted) along the reaction coordinate in the quintet state. The value for Fe is seen to increase from 3.3 to 4.1 in going from RC to TS1, whereas the value for C decreases from 0.0 to −0.5. These values indicate that the formal oxidation state of Fe changes from 4+ to 3+, and the number of unpaired electrons increases from 4 to 5 during the H-abstraction. This electronic reorganization gives rise to an increase in exchange stabilization as H-abstraction progresses and is a typical pattern that has been observed in the exchange-enhanced reactions of high-spin oxoiron(IV) in heme and non-heme systems.[14−17]

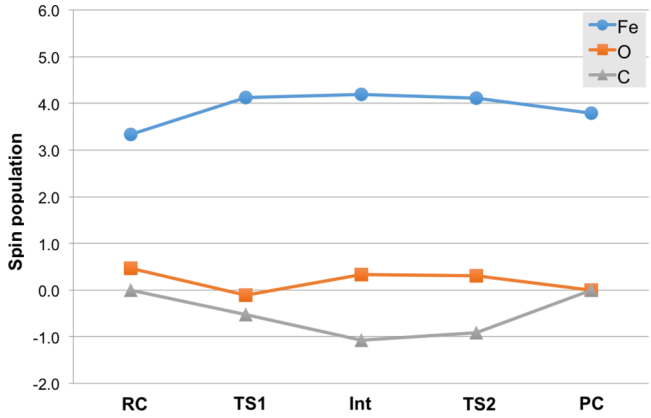

Figure 3. Changes in atomic spin population on Fe, O, and C in the quintet state along the reaction coordinate. The values were obtained with B1.

Xiao et al. showed experimentally that acetaldehyde was also included in the product mixture.[31] Acetaldehyde was formed presumably as a result of the reaction of the above ethanol product with oxoiron(IV). To gain insight into how acetaldehyde is formed, we examined two possible pathways involving initial H-abstraction from the C(1)−H bond and from the O−H bond by oxoiron(IV). Because we have already

DOI: 10.1021/acscatal.5b00475
ACS Catal. 2015, 5, 3287−3291

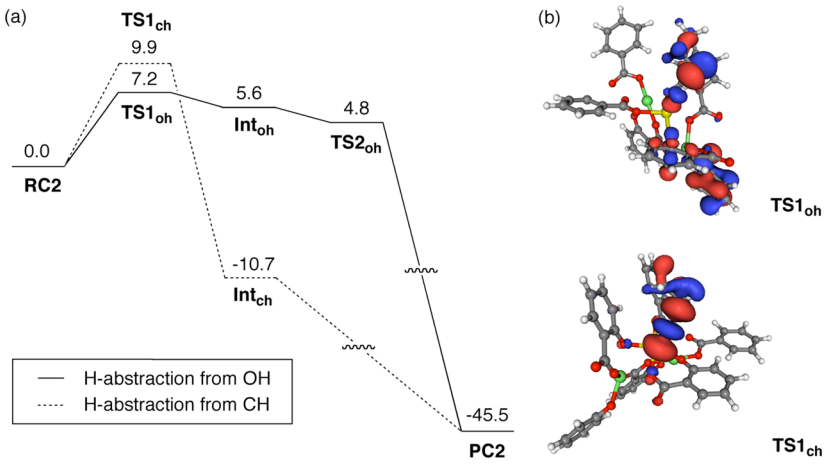

Figure 4. (a) Potential energy diagrams (in kcal/mol) for the reactions between ethanol and the oxoiron(IV) species in the quintet state, as determined at the ONIOM(B3LYP/B2:UFF)//ONIOM(B3LYP/B1:UFF)+ZPE level. (b) B1-calculated SNOs for $TS1_{oh}$ and $TS1_{ch}$.

seen above that the quintet state is much more stable than the triplet state in the reaction of ethane, we considered only the quintet state here. The G4-calculated BDEs for the C(1)−H and O−H bonds of ethanol were 94.5 and 104.1 kcal/mol, respectively (Table S2), indicating that the O−H bond is much stronger than the C−H bond. However, surprisingly, the barrier for H-abstraction from the O−H bond of ethanol (7.2 kcal/mol) was somewhat lower than that for the C−H bond (9.9 kcal/mol) (Figure 4a).

To better understand these results, we further analyzed the spin natural orbitals (SNOs), having an eigenvalue of ∼−1, for the transition states for H-abstraction from the O−H bond ($TS1_{oh}$) and the C−H bond ($TS1_{ch}$). Interestingly, the SNO for $TS1_{oh}$ was not localized on the O−H bond, but it had an amplitude perpendicular to the bond (Figure 4b). Thus, this orbital has a significant character of the oxygen lone-pair orbital, and the transition state is stabilized by the effect of proton-coupled electron transfer (PCET).[50] By contrast, the SNO for $TS1_{ch}$ was well localized on the breaking C−H bond, which suggests that in this case, H-abstraction can be characterized as hydrogen-atom transfer. It is interesting to note that Wang et al. experimentally observed that a synthetic non-heme diiron(IV) complex cleaved the O−H bonds of methanol and *tert*-butyl alcohol rather than their weaker C−H bonds.[51] Our computational results and the PCET scenario appear to be consistent with the experimental trend observed by Wang et al.

Finally, we examined the ethane hydroxylation reactivity of the Fe(III)OH species in Fe-MOF-74 in the sextet spin state. As can be seen in Figure 5, the barrier for H-abstraction by Fe(III)OH is very high (34.9 kcal/mol), much higher than the barrier for oxoiron(IV). Our calculation therefore rules out the possibility that Fe(III)OH acts as a reactive species for the hydroxylation of ethane. We have seen above that the barrier for the reaction of ethane with oxoiron(IV) is reasonably low; however, in the experiment, the reaction yield was not very high. This disparity might be attributed to the fact that the oxoiron(IV) species quickly decays to Fe(III)OH,[31] which is unreactive, as shown here, possibly even before ethane starts to undergo a reaction.

In conclusion, our QM/MM study showed that the ethane hydroxylation in Fe-MOF-74 proceeds in a rebound mechanism on the quintet-state energy surface.[52] The use of the high-spin quintet state makes the barrier for the H-abstraction reaction from the strong C−H bond of ethane reasonably low,

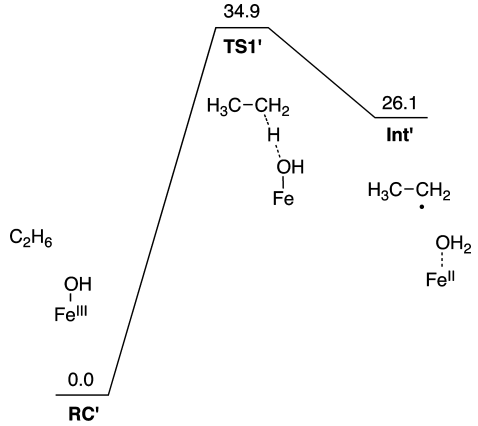

Figure 5. Potential energy diagram (in kcal/mol) for H-abstraction from ethane by Fe(III)OH, as determined at the ONIOM(B3LYP/B2:UFF)//ONIOM(B3LYP/B1:UFF)+ZPE level.

as a result of exchange enhancement at the iron center. The conversion of ethanol to acetaldehyde was also studied, and if oxoiron(IV) acts as the active species here, this reaction is suggested to occur via H-abstraction from the strong O−H bond of ethanol because the transition state for O−H cleavage is stabilized by PCET.

■ ASSOCIATED CONTENT

Supporting Information

The Supporting Information is available free of charge on the ACS Publications website at DOI: 10.1021/acscatal.5b00475.

QM/MM setup, BDE data, raw energy data, examination of other DFT functionals, and XYZ coordinates of optimized geometries.

■ AUTHOR INFORMATION

Corresponding Author

*E-mail: hirao@ntu.edu.sg.

Notes

The authors declare no competing financial interest.

■ ACKNOWLEDGMENTS

H.H. is grateful for a JST-PRESTO grant and a Nanyang Assistant Professorship, and S.B. thanks a Lee Kuan Yew

DOI: 10.1021/acscatal.5b00475
ACS Catal. 2015, 5, 3287−3291

fellowship. We also thank the High Performance Computing Centre at Nanyang Technological University for computer resources.

REFERENCES

(1) Groves, J. T. *J. Inorg. Biochem.* **2006**, *100*, 434−447.
(2) Krebs, C.; Fujimori, D. G.; Walsh, C. T.; Bollinger, J. M., Jr. *Acc. Chem. Res.* **2007**, *40*, 484−492.
(3) *Cytochrome P450: Structure, Mechanism, and Biochemistry*, 3rd ed.; Ortiz de Montellano, P. R., Ed.; Kluwer Academic/Plenum Press: New York, 2005.
(4) Sono, M.; Roach, M. P.; Coulter, E. D.; Dawson, J. H. *Chem. Rev.* **1996**, *96*, 2841−2887.
(5) Denisov, I. G.; Makris, T. M.; Sligar, S. G.; Schlichting, I. *Chem. Rev.* **2005**, *105*, 2253−2277.
(6) Groves, J. T.; Haushalter, R. C.; Nakamura, M.; Nemo, T. E.; Evans, B. J. *J. Am. Chem. Soc.* **1981**, *103*, 2884−2886.
(7) Meunier, B. *Chem. Rev.* **1992**, *92*, 1411−1456.
(8) Nam, W. *Acc. Chem. Res.* **2007**, *40*, 522−531.
(9) Grapperhaus, C. A.; Mienert, B.; Bill, E.; Weyhermüller, T.; Wieghardt, K. *Inorg. Chem.* **2000**, *39*, 5306−5317.
(10) Rohde, J.-U.; In, J.-H.; Lim, M. H.; Brennessel, W. W.; Bukowski, M. R.; Stubna, A.; Münck, E.; Nam, W.; Que, L., Jr. *Science* **2003**, *299*, 1037−1039.
(11) Que, L., Jr. *Acc. Chem. Res.* **2007**, *40*, 493−500.
(12) Biswas, A. N.; Puri, M.; Meier, K. K.; Oloo, W. N.; Rohde, G. T.; Bominaar, E. L.; Münck, E.; Que, L., Jr. *J. Am. Chem. Soc.* **2015**, *137*, 2428−2431.
(13) Kleespies, S. T.; Oloo, W. N.; Mukherjee, A.; Que, L., Jr. *Inorg. Chem.* **2015**, DOI: 10.1021/ic502786y.
(14) Shaik, S.; Hirao, H.; Kumar, D. *Acc. Chem. Res.* **2007**, *40*, 532−542.
(15) Hirao, H.; Kumar, D.; Thiel, W.; Shaik, S. *J. Am. Chem. Soc.* **2005**, *127*, 13007−13018.
(16) Kumar, D.; Hirao, H.; Que, L., Jr.; Shaik, S. *J. Am. Chem. Soc.* **2005**, *127*, 8026−8027.
(17) Hirao, H.; Kumar, D.; Que, L., Jr.; Shaik, S. *J. Am. Chem. Soc.* **2006**, *128*, 8590−8606.
(18) England, J.; Martinho, M.; Farquhar, E. R.; Frisch, J. R.; Bominaar, E. L.; Münck, E.; Que, L., Jr. *Angew. Chem., Int. Ed.* **2009**, *48*, 3622−3626.
(19) England, J.; Guo, Y.; Van Heuvelen, K. M.; Cranswick, M. A.; Rohde, G. T.; Bominaar, E. L.; Münck, E.; Que, L., Jr. *J. Am. Chem. Soc.* **2011**, *133*, 11880−11883.
(20) Lacy, D. C.; Gupta, R.; Stone, K. L.; Greaves, J.; Ziller, J. W.; Hendrich, M. P.; Borovik, A. S. *J. Am. Chem. Soc.* **2010**, *132*, 12188−12190.
(21) Bigi, J. P.; Harman, W. H.; Lassalle-Kaiser, B.; Robles, D. M.; Stich, T. A.; Yano, J.; Britt, R. D.; Chang, C. J. *J. Am. Chem. Soc.* **2012**, *134*, 1536−1542.
(22) Kitagawa, S.; Kitaura, R.; Noro, S.-I. *Angew. Chem., Int. Ed.* **2004**, *43*, 2334−2375.
(23) Zhou, H.-C.; Long, J. R.; Yaghi, O. M. *Chem. Rev.* **2012**, *112*, 673−674.
(24) Gu, Z.-Y.; Park, J.; Raiff, A.; Wei, Z.; Zhou, H.-C. *ChemCatChem* **2014**, *6*, 67−75.
(25) Férey, G. *Chem. Soc. Rev.* **2008**, *37*, 191−214.
(26) Lee, J.; Farha, O. K.; Roberts, J.; Scheidt, K. A.; Nguyen, S. T.; Hupp, J. T. *Chem. Soc. Rev.* **2009**, *38*, 1450−1459.
(27) Yoon, M.; Srirambalaji, R.; Kim, K. *Chem. Rev.* **2012**, *112*, 1196−1231.
(28) Fujita, M.; Kwon, Y. J.; Washizu, S.; Ogura, K. *J. Am. Chem. Soc.* **1994**, *116*, 1151−1152.
(29) Bhattacharjee, S.; Choi, J.-S.; Yang, S.-T.; Choi, S. B.; Kim, J.; Ahn, W.-S. *J. Nanosci. Nanotechnol.* **2010**, *10*, 135−141.
(30) Märcz, M.; Johnsen, R. E.; Dietzel, P. D. C.; Fjellvåg, H. *Microporous Mesoporous Mater.* **2012**, *157*, 62−74.
(31) Xiao, D. J.; Bloch, E. D.; Mason, J. A.; Queen, W. L.; Hudson, M. R.; Planas, N.; Borycz, J.; Dzubak, A. L.; Verma, P.; Lee, K.; Bonino, F.; Crocellà, V.; Yano, J.; Bordiga, S.; Truhlar, D. G.; Gagliardi, L.; Brown, C. M.; Long, J. R. *Nat. Chem.* **2014**, *6*, 590−595.
(32) Choomwattana, S.; Maihom, T.; Khongpracha, P.; Probst, M.; Limtrakul, J. *J. Phys. Chem. C* **2008**, *112*, 10855−10861.
(33) Oxford, G. A. E.; Snurr, R. Q.; Broadbelt, L. J. *Ind. Eng. Chem. Res.* **2010**, *49*, 10965−10973.
(34) Zheng, M.; Liu, Y.; Wang, C.; Liu, S.; Lin, W. *Chem. Sci.* **2012**, *3*, 2623−2627.
(35) Yadnum, S.; Choomwattana, S.; Khongpracha, P.; Sirijaraensre, J.; Limtrakul, J. *ChemPhysChem* **2013**, *14*, 923−928.
(36) Odoh, S. O.; Cramer, C. J.; Truhlar, D. G.; Gagliardi, L. *Chem. Rev.* **2015**, DOI: 10.1021/cr500551h.
(37) Svensson, M.; Humbel, S.; Froese, R. D.; Matsubara, T.; Sieber, S.; Morokuma, K. *J. Phys. Chem.* **1996**, *100*, 19357−19363.
(38) Chung, L. W.; Hirao, H.; Li, X.; Morokuma, K. *Wiley Interdiscip. Rev.: Comput. Mol. Sci.* **2012**, *2*, 327−350.
(39) Chung, L. W.; Sameera, W. M. C.; Ramozzi, R.; Page, A. J.; Hatanaka, M.; Petrova, G. P.; Harris, T. V.; Li, X.; Ke, Z.; Liu, F.; Li, H.-B.; Ding, L.; Morokuma, K. *Chem. Rev.* **2015**, DOI: 10.1021/cr5004419.
(40) Frisch, M. J.; Trucks, G. W.; Schlegel, H. B.; Scuseria, G. E.; Robb, M. A.; Cheeseman, J. R.; Scalmani, G.; Barone, V.; Mennucci, B.; Petersson, G. A.; Nakatsuji, H.; Caricato, M.; Li, X.; Hratchian, H. P.; Izmaylov, A. F.; Bloino, J.; Zheng, G.; Sonnenberg, J. L.; Hada, M.; Ehara, M.; Toyota, K.; Fukuda, R.; Hasegawa, J.; Ishida, M.; Nakajima, T.; Honda, Y.; Kitao, O.; Nakai, H.; Vreven, T.; Montgomery, J. A., Jr.; Peralta, J. E.; Ogliaro, F.; Bearpark, M. J.; Heyd, J.; Brothers, E. N.; Kudin, K. N.; Staroverov, V. N.; Keith, T.; Kobayashi, R.; Normand, J.; Raghavachari, K.; Rendell, A. P.; Burant, J. C.; Iyengar, S. S.; Tomasi, J.; Cossi, M.; Rega, N.; Millam, N. J.; Klene, M.; Knox, J. E.; Cross, J. B.; Bakken, V.; Adamo, C.; Jaramillo, J.; Gomperts, R.; Stratmann, R. E.; Yazyev, O.; Austin, A. J.; Cammi, R.; Pomelli, C.; Ochterski, J. W.; Martin, R. L.; Morokuma, K.; Zakrzewski, V. G.; Voth, G. A.; Salvador, P.; Dannenberg, J. J.; Dapprich, S.; Daniels, A. D.; Farkas, Ö.; Foresman, J. B.; Ortiz, J. V.; Cioslowski, J.; Fox, D. J. *Gaussian 09, Rev. B. 01*; Gaussian, Inc.: Wallingford, CT, USA, 2009.
(41) Becke, A. D. *J. Chem. Phys.* **1993**, *98*, 5648−5652.
(42) Lee, C.; Yang, W.; Parr, R. G. *Phys. Rev. B: Condens. Matter Mater. Phys.* **1988**, *37*, 785−789.
(43) Vosko, S. H.; Wilk, L.; Nusair, M. *Can. J. Phys.* **1980**, *58*, 1200−1211.
(44) Dolg, M.; Wedig, U.; Stoll, H.; Preuss, H. *J. Chem. Phys.* **1987**, *86*, 866−868.
(45) Hehre, W. J.; Radom, L.; Schleyer, P. v. R.; Pople, J. A. *Ab Initio Molecular Orbital Theory*; Wiley: New York, 1986.
(46) Rappé, A. K.; Casewit, C. J.; Colwell, K. S.; Goddard, W. A., III; Skiff, W. M. *J. Am. Chem. Soc.* **1992**, *114*, 10024−10035.
(47) Curtiss, L. A.; Redfern, P. C.; Raghavachari, K. *J. Chem. Phys.* **2007**, *126*, 084108.
(48) Groves, J. T.; McClusky, G. A.; White, R. E.; Coon, M. J. *Biochem. Biophys. Res. Commun.* **1978**, *81*, 154−160.
(49) Cho, K.-B.; Wu, X.; Lee, Y.-M.; Kwon, Y. H.; Shaik, S.; Nam, W. *J. Am. Chem. Soc.* **2012**, *134*, 20222−20225.
(50) Usharani, D.; Lacy, D. C.; Borovik, A. S.; Shaik, S. *J. Am. Chem. Soc.* **2013**, *135*, 17090−17104.
(51) Wang, D.; Farquhar, E. R.; Stubna, A.; Münck, E.; Que, L., Jr. *Nat. Chem.* **2009**, *1*, 145−150.
(52) After submission of this paper, we became aware of the following paper in which the authors presented DFT and ab initio calculations on the oxidation of ethane in $Fe_{0.1}Mg_{1.9}$(dobdc). Verma, P.; Vogiatzis, K. D.; Planas, N.; Borycz, J.; Xiao, D. J.; Long, J. R.; Gagliardi, L.; Truhlar, D. G. *J. Am. Chem. Soc.* DOI: 10.1021/jacs.5b00382.

DOI: 10.1021/acscatal.5b00475
ACS Catal. 2015, 5, 3287−3291